Navigating through the complex transport system: A heuristic approach for city tourism recommendation

Weimin Zheng [a], Zhixue Liao [b,*], Zhibin Lin [c]

[a] *School of Management, Xiamen University, 422 South Siming Road, 361005, Xiamen, China*

[b] *School of Business Administration, Southwestern University of Finance and Economics, 555, Liutai Avenue, 611130, Chengdu, China*

[c] *Durham University Business School, Mill Hill Lane, Durham DH1 3LB, United Kingdom*

** Corresponding author*

E-mail: liaozhixue@swufe.edu.cn

Acknowledgement:

This research received grants from the National Natural Science Foundation of China (No.71971179, No.71701167, No.71601164) and Humanities and Social Science Projects of the Ministry of Education of China (No.17YJC630078).

Navigating through the complex transport system: A heuristic approach for city tourism recommendation

Abstract

The fast development of machine learning and artificial intelligence has led to a great improvement of the smart tourism recommendation system, however many problems associated with the choice of transport modes in city tourism have yet to be solved. This research attempts to address this issue by proposing a model of customized day itineraries with consideration of transport mode choice. With improved particle swarm optimization and differential evolution algorithm, a nondominated sorting heuristic approach was devised. A case study was carried out in Chengdu, China to examine the performance of our approach. The results show that compared with extant methods, our approach achieves better performance. In addition, our approach can create more sensible, multifarious, and customized itineraries than previous methods. Tourism organizations and mobile map app providers could integrate our proposed model into their existing smart service systems, as part of their e-business or digital strategy for enhancing tourist experience.

Keywords: Tourism recommendation system; Smart tourism; City tourism; Transport mode choice; Multi-objective optimization; Nondominated sorting heuristic approach

1 Introduction

It is well recognized in the tourism literature that transport system is essential for tourism development (Kaul, 1985; Prideaux, 2000; Yin, Lin, & Prideaux, 2019). Accessibility or transport infrastructure is one of the crucial destination factors that drive tourist satisfaction and loyalty (Chi & Qu, 2008; Forgas-Coll et al., 2012; Lin, He, & Vlachos Ilias, 2015; Lin, Vlachos, & Ollier, 2018). To access their points of interest within a city destination, tourists may need to navigate through a complex system of different modes of transport, such as metro, light railway, and bus within a city destination (Albalate & Bel, 2010). Despite the vital role of transport system for urban tourism, which substantially contributes to a city's economy (Ashworth & Page, 2011), many metropolitan destinations around the world have experienced various problems such as overcrowded transport systems and traffic congestions (Gronau, 2017), making it difficult for urban tourists to fully enjoy what the city destination has to offer. Both tourism researchers and destination managers are increasingly turning to the latest digital technologies such as the internet of things, big data, machine learning, and artificial intelligence to help enhance tourist experiences (Gretzel, 2011; Gretzel et al., 2015; Tussyadiah, 2020). Thanks to the advances in these digital technologies, smart tourism applications such as tour recommendation systems have made great improvements in recent years (Kotiloglu et al., 2017; Li et al., 2017; Wang et al., 2016).

There are various challenges of designing a tour itinerary in the tour recommendation system, ranging from data sources, data mining methods, tour recommendation algorithms, applications, and performance evaluation (Lim et al., 2019). One of the critical elements in a tourism recommendation system is the tourist trip design problem (TTDP) that plans routes to maximize tourist engagement while considering various constraints (Vansteenwegen & Van Oudheusden, 2007). A TTDP commonly has conflicting objectives, leading to the difficulty of selecting the best option (Rodríguez et al., 2012). Unlike general studies on TTDP, designing tour routes for city tourists requires integrating various transport modes, which is an acknowledged functionality (Garcia et al., 2013). The complex transportation systems (Abbaspour & Samadzadegan, 2011), traffic congestions and tourists' personalized and diversified requirements for transport modes make the TTDP even more complicated (Garcia et al., 2013; Gavalas, Kasapakis, et al., 2015; Gavalas, Konstantopoulos, et al., 2015). There are at least three key modeling challenges that have not been adequately addressed in the literature. First, different transport modes have implications for the amount of travel time required. Second, traffic congestion has different impacts on travel time depending on the transport mode used; thus, the degree of uncertainty about travel time is different across different transport modes. Third, tourists have different attitudes toward uncertainty or risk.

This study therefore aims to address the above three key challenges by proposing a model of customized day itineraries for city tourists while considering transport mode choice (TTDP-TMC). In particular, a couple of conflicting objectives (utility and risk) and many constraints associated with attractions, tourists, and urban transportation networks are considered. The Pareto optimality definition is adopted and a nondominated sorting heuristic approach (NSHA) is designed with improved particle swarm optimization (PSO) and a differential evolution algorithm (DEA). This approach is distinct from extant methods in four major aspects. (1) Solutions are coded using a triple-layer, variable-length asymmetric chromosome. (2) The designed method optimizes solutions that involve continuous and discrete variables merging improved PSO and DEA. (3) A random simulation-based method combining the Pareto optimality definition is proposed to handle time-dependent stochastic variables (TDSVs). (4) A hybrid evolution structure is designed to improve evolutionary efficiency. A case study in Chengdu, an old but modernized city in the Sichuan Province of China, was conducted to confirm this approach's validity.

This study makes a major methodological contribution to the tourism recommendation systems literature, which also has valuable practical implications. In the methodological front, we develop a novel model for tourist trip design considering the complex transport system in a metropolitan city context. On the managerial front, our model provides tourism organizations with insights into improving their recommendation services that are practical and useful for their customers. The rest of this study is structured as follows. Related literature on TTDP is briefly reviewed in Section 2. The mathematical TTDP-TMC model for city tourists is described in Section 3, and our approach is introduced in Section 4. The case study that is used to validate the NSHA performance is discussed in Section 5. Finally, Section 6 concludes and suggests further research directions.

2 Literature review

2.1 Transport and tourist decision making

Organizing an excursion trip within a city destination is a complex task for the tourists (Kotiloglu et al., 2017; Pellegrini & Scagnolari, 2019). They have to make decisions on the places to visit and activities based on their location of accommodation, available means of transport, duration of stay, and monetary budget, which are the major constraints they have to take into consideration. Decisions on places to visit (movements) and how to access to the places of interest (transport choice) are inter-related (Le-Klähn et al., 2015; Masiero & Zoltan, 2013). On the one hand, tourist decisions on their activities and places to visit are influenced by the transport system (Prideaux, 2000); and on the other hand, tourist characteristics, motivations, and trip profile influence their choice of transport mode (Hyde & Laesser, 2009), and the resultant tourist spatial-temporal movements could then influence the city's transport planning decisions (Lew & McKercher, 2006). Previous studies have shown that both the places to be visited and the transport mode used are determined by many factors such as tourist origin (Debbage, 1991), cultural background (Dejbakhsh, Arrowsmith, & Jackson, 2011), personality (Plog, 2002), special interests (Fennell, 1996), familiarity with the destination (McKercher et al., 2012), length of stay (Xia et al., 2010), and motivational variables (Masiero & Zoltan, 2013).

In recent years, recommendation systems have been widely used in e-business context, where online venders such as Amazon and Netflix provide their customers with the information of products or services that closely match their individual preferences (Lee & Hosanagar, 2019). When organizing a day trip within a city destination, some tourists may turn to travel agencies, hotels and visitor centers for advice and many others tend to search online social media for information and inspirations. However, tourists could be information over-loaded and reach a suboptimal trip plan (Zheng et al., 2020). Technology-savvy tourists now turn to smart tourism applications for trip planning (Kotiloglu et al., 2017). Using sophisticated algorithms based on data collected from various sources, a smart tourism recommendation system helps tourists to maximize their experience efficiently and cost-effectively (Lim et al., 2019; Vansteenwegen & Van Oudheusden, 2007; Wong & McKercher, 2012).

2.2 Tourist trip design problem

Previous studies have contributed to the improvement of customized tourism products, however, transport mode choice has received limited attention despite being one of the most appreciated functionalities (Albalate & Bel, 2010; Garcia et al., 2013). TTDP for city tourists are more complex because the metropolitan transit networks are complicated (Garcia et al., 2013; Gavalas, Kasapakis, et al., 2015; Gavalas, Konstantopoulos, et al., 2015). In addition, tourists may have various requirements or preferences for transport modes: For instance, some tourists may be flexible with transport modes, whereas others might specify all or some of the transport modes for their trip. The existing methods cannot be directly used to solve the TTDP with consideration of the transport mode choice within a city.

There are three main problems associated with the TTDP for city tourists that yet to be solved. First, different transport modes inevitably result in varying travel time, which in turn affects attraction selection, sequencing, and time allocation. For example, riding a taxi tends to consume less travel time than riding the subway, thus allowing tourists to spend more time in tourist attractions or visit more attractions to achieve greater utility. Considering transport mode choice in TTDP not only adds a decision variable but also creates a subversive impact on the overall optimization structure. This is because attraction selection, sequencing, time allocation, and transport mode are factors that affect and restrict each other.

Second, traffic congestion has become a daily phenomenon in cities, resulting in uncertain travel times between attractions (Verbeeck, Vansteenwegen, & Aghezzaf, 2016). Realizing this issue, travel time has been modeled as a time-dependent variable that changes based on departure time (Abbaspour & Samadzadegan, 2011; Garcia et al., 2013; Gavalas, Konstantopoulos, et al., 2015). Apart from being time-dependent, travel time is stochastic due to many variables (e.g., weather, congestion, and accidents), making the accurate estimation of arrival time at the destination challenging (Verbeeck et al., 2016). Research on TTDP in an urban setting thus involves a stochastic environment that depends on time. Liao and Zheng (2018) first designed customized day itineraries in such an environment. The problem raised in the present study is more complicated than the TTDP proposed by Liao and Zheng (2018) owing to the various effects of traffic congestion on different transport modes. Consequently, travel time is heavily dependent on transport mode choice. For example, compared with taxis, subway or shared bicycles have relatively lower uncertainty of travel time.

Third, due to this effect of transport mode choices on travel time uncertainty, designing personalized tour routes for city tourists must consider not only the travel utility but also the risk. Measured in probability terms, risk is the conservative estimate of completing a trip within the allocated time (Liao & Zheng, 2018). Depending on tourists' attitude toward risk, they may prefer a route with greater utility despite the higher probability of failure to finish a trip within the allocated time, or a more leisurely trip with lower utility (Lau et al., 2012). This consideration changes our TTDP into a multi-objective optimization problem (MOP), that is, two potentially conflicting objectives (utility and risk) should provide a beneficial trade-off according to the tourist characteristics (e.g., preferences and attitude toward risk).

In this study, we propose a TTDP-TMC that optimizes the interactive decision variables, including attraction selection, sequencing, time allocation, and transport mode choice. In addition, the involvement of discrete and continuous variables increases the difficulty of optimization (Liao & Zheng, 2018; Zheng et al., 2020; Zheng & Liao, 2019; Zheng, Liao, & Qin, 2017). Our TTDP-TMC is in a stochastic environment dependent on time with many variables (TDSVs). As a decision variable, transport mode choice affects the environment uncertainty. Finally, considering the differences in tourists' attitudes toward risk, our TTDP-TMC requires a beneficial trade-off between utility and the risk. A single-objective optimization problem then becomes a multi-objective optimization problem (MOP).

3 Methodology

A mathematical model is presented in this section to describe our TTDP-TMC. Table 1 lists the mathematical variables and their definitions. The first and second subsections discuss the objectives and constraints of the mathematical model, respectively.

Table 1. Mathematical notations and descriptions

Variable	*Description*
$\boldsymbol{V}$	Urban destination vertices
$\boldsymbol{V_A}$	Urban destination attractions
$\boldsymbol{V_I}$	Starting locations
$\boldsymbol{V_F}$	Final arrival locations
N	Number of vertices
τ	Planned start time of the trip
n_i	Discrete visits to vertex v_i
M	Total stages, that is, the sum of n_i, $M = \sum n_i$, $i = 1, 2, \ldots, N$
t_i	Average time spent by tourists at v_i
Λ_j	Vertex visited at jth stage, $j=1, 2, \ldots, M$
T_{max}	Budgeted time allotted to the tourist
$\left[t_i^o, t_i^c\right]$	v_i Time window
TS_q	qth timeslot, $q=1, 2, \ldots, Q$
$\mathrm{E}_q\left(\Lambda_j, \Lambda_{j+1}\right)$	Transport modes for TS_q between Λ_j and Λ_{j+1}
p_i	Tourist preference value for v_i, $p_i \in [0, 1]$
β	Tourist attitude toward risk, $\beta \in [0, 1]$
$\tilde{t}_q^k\left(\Lambda_j, \Lambda_{j+1}\right)$	Travel time required between vertices (Λ_j, Λ_{j+1}) for TS_q using kth transport mode
$\utilde{t}_j^a$	Time of arrival at vertex Λ_j
$\utilde{t}_j^s$	Start time of actual visit at vertex Λ_j
$\utilde{t}_j^e$	Time of departure from vertex Λ_j
$\utilde{u}_j$	Utility gained at jth stage
$\utilde{U}$	Total utility gained from the entire trip
d_j	Duration of time spent at the visited vertex at jth stage
x_{ij}	If v_i is visited at jth stage, then set $x_{ij}=1$; otherwise, $x_{ij}=0$
$y^k\left(\Lambda_j, \Lambda_{j+1}\right)$	If kth transport mode is chosen from Λ_j to Λ_{j+1}, then set 1; otherwise, 0

3.1 Model objectives

This study intends to come up with personalized day tour routes, represented in a mathematical model of a multiple-objective TTDP set in a time-dependent stochastic environment. To be specific, route spatial-temporal structures and transport mode choice are optimized. In addition, an advantageous trade-off is reached between utility and risk within an allocated time (T_{max}). Popular vertices may have repeat visits (Tsai & Chung, 2012), so we used n_i to represent the number of discrete visits to v_i. The entire trip is then divided into M stages with N as the number of vertices in the destination, as expressed in Eq. (3.1).

$$M = \sum_{i=1}^{N} n_i \tag{3.1}$$

At each stage, the utility gained depends on the visited vertex (Λ_j). Specifically, the utility depends on the personal preference (p_i) of the tourist for Λ_j and the actual time spent at Λ_j (Zheng et al., 2017). Rather than constant, the utility associated with each vertex is a diminishing time function, because marginal subjective sensations ($MS_i(t)$) typically decreases with time spent at the same vertex (Liao & Zheng, 2018; Zheng et al., 2017). On the basis of these considerations, Eq. (3.2) calculates the utility gained at the jth stage under the assumption that no utility is gained while in transit and during waiting times. Eq. (3.3) follows and maximizes the total utility gained from the entire trip, which is the first objective of the TTDP-TMC.

$$\tilde{u}_j = \int_{\tilde{t}_j^s}^{\tilde{t}_j^e} \left\{ \sum_{i=1}^{N} \left[MS_i(t) \cdot p_i \cdot x_{ij} \right] \right\} \mathrm{d}t \tag{3.2}$$

$$U = \sum_{j=1}^{M} \tilde{u}_j \tag{3.3}$$

In Eq. (3.2), $MS_i(t)$ is obtained from v_i at moment t, a non-negative diminishing time function. x_{ij} is a 0–1 discrete variable, that is, if v_i is visited at the jth stage, then set $x_{ij}=1$; otherwise, $x_{ij}=0$. At vertex Λ_j, $\tilde{t}_j^a$ is the time of arrival and $\tilde{t}_j^s$ is the actual start time of the visit. Of note, in numerous instances, $\tilde{t}_j^a$ is not the same as $\tilde{t}_j^s$, due to waiting or other activities required at a given vertex. Thus, Eq. (3.4) computes $\tilde{t}_j^s$ as follows:

$$\tilde{t}_j^s = \max\left[\tilde{t}_j^a, t_i^o \right] \tag{3.4}$$

Calculating $\tilde{t}_j^a$ is more complicated than $\tilde{t}_j^s$, because $\tilde{t}_q^k(\Lambda_j, \Lambda_{j+1})$ depends not only on the distance between Λ_j and Λ_{j+1}, but also on the transport mode choice. In addition, as TDSVs, $\tilde{t}_q^k(\Lambda_j, \Lambda_{j+1})$ follow varied distribution functions in different timeslots. Liao and Zheng (2018) present the detailed calculation of $\tilde{t}_j^a$.

$\tilde{t}_j^a$, $\tilde{t}_j^s$ and $\tilde{t}_j^e$ are TDSVs, whereas $\tilde{u}_j$ and $\tilde{U}$ falls under TDSVs. The direct evaluation of their performance cannot be attained, so these stochastic variables require conversion into deterministic variables. Conversion can be achieved through any of three main models, namely, probability maximization model (P-model), expectation optimization model (E-model), and variance minimization model (V-model) (Liao & Zheng, 2018). By using an expected value, the E-model can efficiently manage the stochastic objective functions. On the basis of the E-model, the objective function in Eq. (3.3) can then be used in Eq. (3.5), where $E\left|\tilde{u}_j\right|$ is the expected utility at the *j*th stage.

$$f_1 \qquad Max \quad U = \sum_{j=1}^{M} E\left|\tilde{u}_j\right| \tag{3.5}$$

Apart from utility, the route risk should be considered. Measured in probability terms, risk is the conservative estimate of completing the tour within the allocated time. Tour route design should minimize a certain perception of risk. The P-model can effectively consider the user's risk profile and, thus, is employed to minimize the probability of failing to complete the tour within the allocated time. In Eq. (3.6), $\tilde{t}_M^a$ reflects the end of the trip as the time of arrival at A_M, and $Ch\{A \le B\}$ means the confidence level meets the condition $A \le B$.

$$f_2 \qquad Min \quad R = 1 - Ch\left\{\tilde{t}_M^a \le \tau + T_{\max}\right\} \tag{3.6}$$

3.2 Model constraints

Designing personalized tour routes should address two types of constraints, namely, customized and permanent technical constraints. Permanent technical constraints ensure the validity of routes as well as their practical meaning, whereas the customized constraints restrict a tourist's specific requirements to be incorporated into the model (Rodríguez et al., 2012).

In a tour, the first stage involves the tourist departing from a starting location, and the last stage involves the final arrival at an end destination, as given in Eq. (3.7). From the second to the *M-1*th stage, Eq. (3.8) guarantees that only one attraction is visited. In these equations, V_I, V_F, and V_A represent the starting locations, final arrival locations, and tourist attractions, respectively. Similarly, Eq. (3.9) ensures that each stage involves taking only one transport mode.

$$\sum_{v_i \in V_I} x_{i1} = \sum_{v_j \in V_F} x_{jM} = 1 \tag{3.7}$$

$$\sum_{v_i \in V_A} x_{ij} = 1,\ j = 2, 3, \cdots, M-1 \tag{3.8}$$

$$\sum_{k \in \mathrm{E}_q(\Lambda_j, \Lambda_{j+1})} y^k\left(\Lambda_j, \Lambda_{j+1}\right) = 1, \forall \Lambda_j, \Lambda_{j+1} \in V,\ j = 1, 2, \cdots, M-1 \tag{3.9}$$

Time and path connectivity are obtained in Eqs. (3.10) and (3.11), where z_{ij} is a 0–1 discrete variable. If v_i and then v_j are visited, then $z_{ij}=1$; 0, otherwise.

$$\tilde{t}_j^{\,e} + \tilde{t}_q^{\,k}\left(\Lambda_j, \Lambda_{j+1}\right) = \tilde{t}_{j+1}^{\,a}, \left(\forall j = 1, 2, \cdots, M-1\right) \tag{3.10}$$

$$\sum_{v_i \in V_I \cup V_A} z_{ij} = \sum_{v_k \in V_A \cup V_F} z_{jk}, \forall v_j \in V_A; v_i \neq v_j, v_j \neq v_k \tag{3.11}$$

In addition, personalized constraints require incorporation into the model. Before starting their trips, tourists often create a list of "must-visit" or "must-avoid" vertices and have a time budget. Tourists may feel hurried if time constraints are disregarded. If the trip includes unwanted vertices or excludes favorite ones, then the tourism experience can be clearly affected (Tsai & Chung, 2012). To prevent these scenarios, Eqs. (3.12) and (3.13) ensure that compulsory vertices $\boldsymbol{S_C}$ are included in the trip and that the vertices to be avoided $\boldsymbol{S_A}$ are excluded, respectively.

$$\sum_{j=1}^{M} x_{ij} \geq 1, if\ v_i \in \boldsymbol{S_C} \tag{3.12}$$

$$\sum_{j=1}^{M} x_{ij} = 0, if\ v_i \in \boldsymbol{S_A} \tag{3.13}$$

4 Solution algorithm

Our TTDP-TMC is novel and challenging, because it is a generalization of the OP, but much more complex. Spatial-temporal routes and transport mode choice require optimization, and an advantageous trade-off must be gained between utility and risk in a time-dependent stochastic environment. TDSVs also adhere to varying types of distribution functions. Three steps were taken to address these challenges. (1) the Pareto optimality was adopted to effectively address MOPs (Chen, Zhou, & Xiang, 2017). (2) A random simulation-based method was employed to manage TDSVs. Finally, (3) solutions with continuous and discrete variables were optimized merging improved PSO and DEA. The overall NSHA framework is illustrated in Fig. 1, which comprises initialization, random simulation, and hybrid evolution.

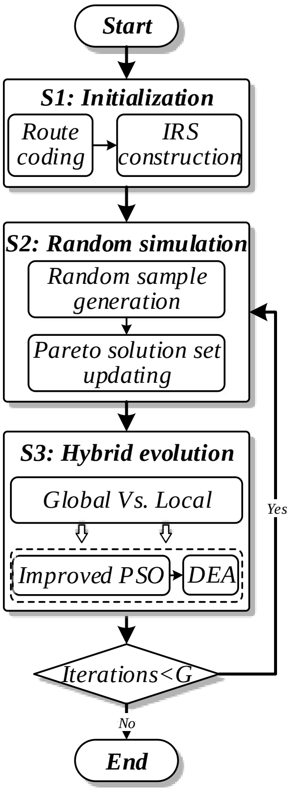

Fig. 1. Methodological framework

Initialization involves route coding with a triple-layer, variable-length asymmetric chromosome, and an initial route set (***IRS***) is constructed using an improved greedy algorithm. In a random simulation, random samples are generated to determine the feasible solutions, on the basis of which a Pareto solution set is produced. Finally, the feasible solutions follow a hybrid evolution strategy that merges the improved PSO and DEA. Upon reaching the maximum number of iterations (G), a critical parameter that needs to be determined on the basis of the convergent situation, the algorithm stops. The end of each iteration generates a new Pareto-optimal set (***POS***), and the last iteration ***POS*** is the output.

4.1 Initialization

The majority of evolution algorithms require advanced determination of the solution dimensions (Zheng et al., 2017), which cannot be applied to the present problem due to possible variations in the vertices that a tourist visits. To code the route, Zheng et al. (2017) designed a double-layer, variable-length chromosome that involves the spatial structure of the route (vertex selection and sequencing) and the time spent at each chosen vertex. However, this study optimizes the spatial-temporal structure and transport mode of the route. A triple-layer, variable-length, asymmetric chromosome is introduced to code the routes. The upper layer is the route's spatial structure, the middle layer denotes the transport modes selected among vertices, and the lower layer indicates the time spent at a certain vertex. This route coding is illustrated with an example in Fig. 2, which depicts that the tourist starts the trip at v_5, then successively visits v_2, v_1, v_7, v_8, v_1, and v_9, where the trip ends. At these vertices (v_2, v_1, v_7, v_8, and v_1), the values of time spent are 10, 15, 8, 20, and 30 minutes. The chosen transport modes between vertices are 1 (taxi), 1, 2 (subway), 3 (bus), 2, and 3, successively.

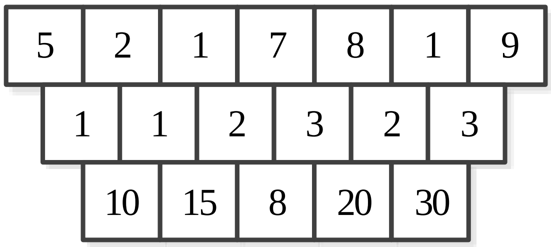

Fig. 2. Example of route coding

The ***IRS*** quality strongly influences the model performance. In traditional route optimization methods, the ***IRS*** is constructed using the random or the greedy approach. In this study, the ***IRS*** is generated through a greedy algorithm improved by Zheng et al. (2017) to gain an advantageous trade-off between quality and diversity.

4.2 Random simulation

In this step, a ***POS*** is generated. However, generating a fixed feasible region is impossible because our TTDP-TMC is set in a time-dependent stochastic environment and involves TDSVs. Therefore, a set of random samples for the TDSVs must first be generated, and then the corresponding solutions are identified by adopting the Pareto optimality definition.

4.2.1 Generating random samples

Travel times ($\tilde{t}_q^k\left(v_i, v_j\right)$) between vertices ($v_i$, v_j) using the kth transport mode for TS_q are TDSVs, and they adhere to different distribution functions depending on timeslots. Employing the distribution fitting tool in the MATLAB software package, considerable historical data are used to fit these distribution functions. On the basis of which, $\tilde{t}_q^k\left(v_i, v_j\right)$ of each timeslot are generated for the fth random sample (refer to Eq. (4.1)). The travel times between vertices (v_i, v_j) by different transport modes can be denoted as an array, as shown in Eq. (4.2). Afterward, an $F \times Q$ matrix (**Matrix** ($\mathbf{M}[t]$) is constructed, as expressed in Eq. (4.3), where F is the number of random samples and Q is that of timeslots. F is highly and positively correlated with the algorithm's performance but highly and negatively correlated with its efficiency.

Determining the best value for F is important to balance performance and efficiency.

$$\mathbf{M}\left[t_q^{k,f}\right]=\begin{bmatrix} t_q^{k,f}\left(v_1,v_1\right) & t_q^{k,f}\left(v_1,v_2\right) & \cdots & t_q^{k,f}\left(v_1,v_N\right) \\ t_q^{k,f}\left(v_2,v_1\right) & t_q^{k,f}\left(v_2,v_2\right) & \cdots & t_q^{k,f}\left(v_2,v_N\right) \\ \vdots & \vdots & \ddots & \vdots \\ t_q^{k,f}\left(v_N,v_1\right) & t_q^{k,f}\left(v_N,v_2\right) & \cdots & t_q^{k,f}\left(v_N,v_N\right) \end{bmatrix} \tag{4.1}$$

$$\mathbf{A}\left[t_q^f\right]=\left[\mathbf{M}\left[t_q^{1,f}\right] \quad \mathbf{M}\left[t_q^{2,f}\right] \quad \cdots \quad \mathbf{M}\left[t_q^{K,f}\right]\right] \tag{4.2}$$

$$\mathbf{Matrix}\left(\mathbf{M}[t]\right)=\begin{bmatrix} \mathbf{A}\left[t_1^1\right] & \mathbf{A}\left[t_2^1\right] & \cdots & \mathbf{A}\left[t_Q^1\right] \\ \mathbf{A}\left[t_1^2\right] & \mathbf{A}\left[t_2^2\right] & \cdots & \mathbf{A}\left[t_Q^2\right] \\ \vdots & \vdots & \ddots & \vdots \\ \mathbf{A}\left[t_1^F\right] & \mathbf{A}\left[t_2^F\right] & \cdots & \mathbf{A}\left[t_Q^F\right] \end{bmatrix} \tag{4.3}$$

4.2.2 Updating the Pareto solution set

F random samples are generated according to the distribution functions. Then, each solution's objective values (utility and risk) are calculated for each random sample based on Eqs. (3.5) and (3.6). The solution utility for f random samples can be calculated according to Eq. (4.4), whereas the total solution utility equals the average of all random samples' utilities, as shown in Eq. (4.5). To calculate the solution risk, a 0–1 discrete variable α^f is defined to determine whether the trip is completed within the time allocation, as shown in Eq. (4.6), where $t_M^{a,f}$ denotes the completion time of the trip. Finally, the solution risk can be calculated following Eq. (4.7).

$$u_j^f=\int_{t_j^{s,f}}^{t_j^{e,f}}\left\{\sum_{i=1}^{N}\left[MS_i\left(t\right)\cdot p_i\cdot x_{ij}\right]\right\}\mathrm{d}t,\left(\forall f=1,2,\cdots,F\right) \tag{4.4}$$

$$U=\frac{1}{F}\sum_{f=1}^{F}\sum_{j=1}^{M}u_j^f \tag{4.5}$$

$$\alpha^f=\begin{cases}1, t_M^{f,a}\le\tau+T_{\max}\\ 0, t_M^{f,a}>\tau+T_{\max}\end{cases} \tag{4.6}$$

$$R=\frac{1}{F}\sum_{f=1}^{F}\alpha^f \tag{4.7}$$

With a number of conflicting objectives, MOPs have no single optimization solution for all the objectives. For our TTDP-TMC, a single route cannot maximize utility and minimize risk at the same time. To solve this, we balance these two objectives by searching for a set of routes that is based on Pareto theory. The following Pareto-related values are defined with reference to Zheng and Liao (2019).

Definition 1. (***Pareto dominance***): For any two routes x and y (x, $y \in \boldsymbol{R^n}$), if $\left(\forall i \in \{1,2,\cdots n\}: f_i(x) \geq f_i(y)\right) \wedge \left(\exists j \in \{1,2,\cdots n\}: f_i(x) > f_i(y)\right)$, then route x considered to dominate route y ($x \succ y$).

Definition 2. (***Pareto-optimal route***): For any route y ($y \in \Omega$) that does not dominate route x. Route x is considered as a Pareto-optimal route (denoted as *PR*) if and only if $\neg\exists y \in \Omega : y \succ x$.

Definition 3. (***Pareto-optimal set***): All *PRs* are included in a ***POS*** (denoted as $\boldsymbol{POS} = \{x | \neg\exists y \in \Omega : y \succ x\}$).

Definition 4. (***Pareto-optimal front***): Every objective function value corresponding to the *PRs* in ***POS*** is included in the Pareto-optimal front (denoted as $\boldsymbol{PF} = \left\{F(x) = \left(f_1(x), f_2(x), \cdots, f_n(x)\right)^T | x \in \boldsymbol{POS}\right\}$).

Each of the iterations generates a set of routes. The generated set of routes is denoted as *S(g)* at the *g*th iteration, and the ***POS*** of the previous iteration is ***POS****(g−1)*. The ***POS*** updating is illustrated in Fig. 3 using the pseudo-code definitions. Given ***POS****(g−1)*, *S(g)*, and population size (*P*), the output is ***POS(g)*** (Fig. 3, lines 1–2). ***POS(g)*** is initially an empty set, and its number of *PRs* is parameter *n* (Fig. 3, lines 3–4). The entire updating process is depicted in Fig. 3 (lines 5–22). First, *S(g)* and ***POS****(g−1)* are combined to derive a candidate route set (***CRS***). If the number of *PRs* in ***CRS*** is less than *P*, then the following operations need repeating: *PRs* are screened from ***CRS*** according to **Definition 1** to generate a new set (S_N), and *m* is the number of *PRs* in S_N (lines 7–8 in Fig. 3). If the number of *PRs* in ***POS(g)*** and S_N is less than *P* ($n + m \leq P$), then all *PRs* in S_N are inserted into ***POS(g)*** and removed from ***CRS*** accordingly. The ***CRS***, ***POS(g)***, and *n* are then updated (lines 9–12 in Fig. 3). If the number of *PRs* in ***POS(g)*** and S_N exceeds *P* ($n + m > P$), then the distance between the risk of each PR_i (f_2) in S_N and the tourist's attitude toward risk (β) is obtained by Eq. (4.8). The *PRs* with the shortest distances are selected and inserted into ***POS(g)*** until it equals *P* or all *PRs* in S_N have been moved to ***POS(g)*** (lines 13–21 in Fig. 3). The process stops when the number of *PRs* in ***POS(g)*** equals *P* ($n = P$). The output of random simulation is a ***POS***, which serves as input for hybrid evolution.

$$\pi = \left| f_2 - \beta \right| \tag{4.8}$$

Pareto-optimal set updating

Input: $\boldsymbol{POS}(g\text{-}1)$, $S(g)$, P;
Output: $\boldsymbol{POS}(g)$;
Set $\boldsymbol{POS}(g)$ = [ ];
Set $n = |\boldsymbol{POS}(g)|$;
Combine $S(g)$ with $\boldsymbol{POS}(g\text{-}1)$ to obtain $\boldsymbol{CRS}$
while $\{n \leqslant P\}$
  Extract PRs from $\boldsymbol{CRS}$ to generate S_N;
  Set $m=|S_N|$;
  if $n+m \leq P$ **then**
    Insert ($\boldsymbol{POS}(g)$, S_N);
    Remove S_N from $\boldsymbol{CRS}$;
    Update $\boldsymbol{CRS}$, $\boldsymbol{POS}(g)$, n;
  else
    Calculate π_i for $PR_i \in S_N$;
    Sort $PRs \in S_N$ by π_i in ascending order;
    for $i=1$ to **min** (m, P-n) **do**
      Insert ($\boldsymbol{POS}(g)$, PR_i);
      Remove PR_i from $\boldsymbol{CRS}$;
    end for;
    Update $\boldsymbol{CRS}$, $\boldsymbol{POS}(g)$, n;
  end if;
end while;
Return $\boldsymbol{POS}(g)$.

Fig. 3. Updating of Pareto-optimal set

4.3 Hybrid evolution

4.3.1 Improved particle swarm optimization

In this step, the evolution aims to evaluate the Pareto solutions in ***POS*** and generate routes with a greater trade-off between utility and risk. As previously discussed, the solution is coded as a triple-layer chromosome that shows, from top to bottom, the spatial structure of the route, choice of transport mode, and the time spent at corresponding vertices. The first two are discrete decision variables, whereas the last is continuous. With such decision variables, Zheng and Liao (2019) optimized multi-objective solutions by merging ant colony optimization (ACO) and DEA. Apart from the above study, very limited research discusses the optimization of multi-objective solutions with continuous and discrete decision variables. Although ACO possesses good robustness and searching ability, it exhibits several flaws, such as slow convergence that is easily trapped into the local optimum (Dorigo & Blum, 2005). Although combining ACO and DEA offers a different perspective, this method cannot solve multiple TDSVs efficiently and, thus, is not applicable for the time-dependent stochastic TTDP. We simulate a set of random samples that can increase computation complexity and result in poor algorithm efficiency to effectively handle TDSVs. For instance, computation complexity increases to approximately F times its value without TDSVs if F is the number of random samples. The efficiency of evolutionary operators considerably affects the algorithm performance for TTDP-TMC.

By contrast, PSO, which was originally attributed to Kennedy and Eberhart (1995), is ideally situated for the present problem due to its higher search efficiency (Bonyadi & Michalewicz, 2017; Poli, 2008). The PSO algorithm employs a population (swarm) of possible solutions (particles), which moves with the guidance of their own and the swarm's best-known positions in the search-space. Thus, the discovery of improved positions then adds to guiding the swarm movements. These evolution processes are illustrated in Eqs. (4.9) and (4.10), where x_j^t and x_j^{t+1} represent the jth particle's current solution and next iteration solution, respectively. v_j^{t+1} is the movement velocity to transition from x_j^t to x_j^{t+1}, which can be calculated according to Eq. (4.9), where $Pbest_j^t$ indicates the jth particle's best known solution, whereas $Gbest^t$ denotes the entire swarm's best-known solution. ω means inertia weight, whereas σ_1 and σ_2 are learning factors that control the particles' learning intensity to individual optimum and global optimum, respectively.

$$x_j^{t+1} = x_j^t + v_j^{t+1} \tag{4.9}$$

$$v_j^{t+1} = \omega v_j^t + \sigma_1\left(Pbest_j^t - x_j^t\right) + \sigma_2\left(Gbest^t - x_j^t\right) \tag{4.10}$$

Although PSO is well-known for superior search efficiency, its defects are similarly widely realized to include precocious convergence and poor local optimization (Bonyadi & Michalewicz, 2017; Poli, 2008). By contrast, the genetic algorithm (GA) is known to be robust. It does not need auxiliary knowledge, and it presents many advantages in solution methodology and optimization performance. Thus, this algorithm offers wide applicability to optimization problems that are discrete (Osman, Abo-Sinna, & Mousa, 2005). Essentially, PSO learning operators can be regarded as the evolutionary strategies of GA, in which $Pbest_j^t$ and $Gbest^t$ are the "parents". Therefore, in optimizing the discrete variables, our approach designs the improved PSO by combining the GA optimization concept. The improved PSO is illustrated with a specific example in Fig. 4. First, the current solution of the jth particle (x_j^t) $Pbest_j^t$, and $Gbest_j^t$ are determined in Fig. 4(a), and their upper two chromosome layers are used as parents. Second, a two-point mutation converts x_j^t to

$\boldsymbol{M}\left[x_j^t\right]$, while a single-point crossover is implemented between x_j^t and $Pbest_j^t$ and between x_j^t and $Gbest^t$ to generate $\boldsymbol{C}\left[x_j^t, Pbest_j^t\right]$ and $\boldsymbol{C}\left[x_j^t, Gbest^t\right]$, as shown in Fig. 4(b)–(c). Finally, the new solution (named the offspring) is generated using a three-segment combination. (1) Two points in $\boldsymbol{M}\left[x_j^t\right]$ are randomly selected to divide into three segments, and similar operations are conducted in $\boldsymbol{C}\left[x_j^t, Pbest_j^t\right]$ and $\boldsymbol{C}\left[x_j^t, Gbest^t\right]$, as shown in Fig. 4(c). (2) The offspring (x_j^{t+1}) is determined as concatenation of parts from $\boldsymbol{M}\left[x_j^t\right]$, $\boldsymbol{C}\left[x_j^t, Pbest_j^t\right]$, and $\boldsymbol{C}\left[x_j^t, Gbest^t\right]$, as shown in Fig. 4(d).

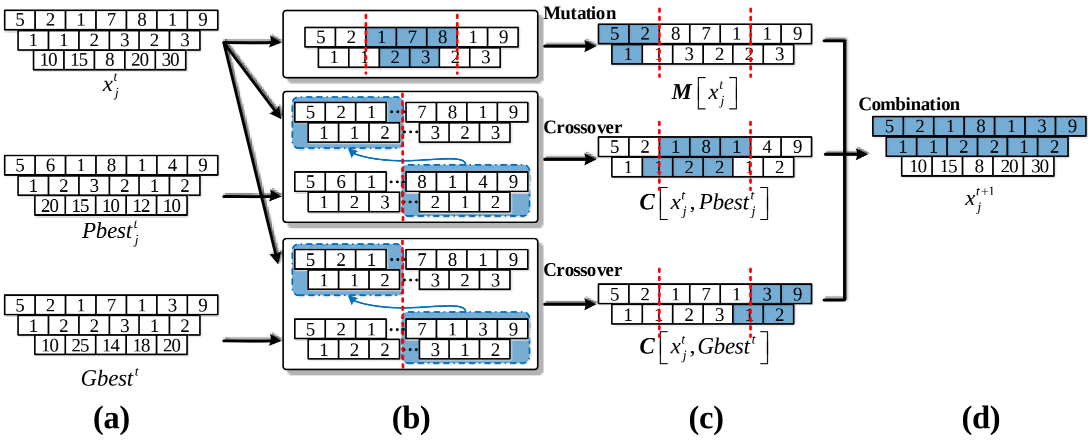

Fig. 4 Improved PSO

Upon the optimization of the route's spatial structure and transport mode choice, another task must be completed to obtain the time consumed at the corresponding vertices, which is a continuous decision variable. This task optimizes the evolution results of the improved PSO by introducing a DEA, which then relies on crossover, mutation, and selection (Zheng et al., 2017) .

4.3.2 Hybrid evolution structure

In addition to the improved evolutionary operators, the hybrid evolution structure proposed by Liao and Zheng (2018) is adopted to further increase evolutionary efficiency. In the hybrid evolution structure, the solution evolution can be considered predatory global and local searches for solution space. The global search explores new local solution space, whereas the local search obtains enhanced quality of results (Parouha & Das, 2016).

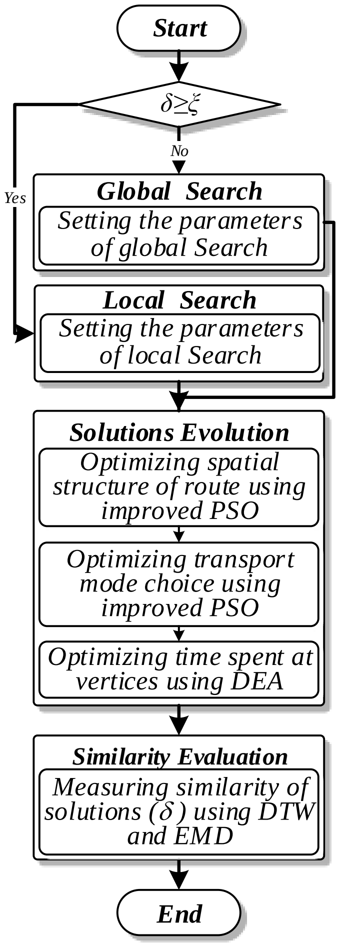

Fig. 5. Hybrid evolution procedure

In accordance with the TTDP-TMC, the TTDP evolution aims to generate routes with improved performance. Route performance is associated with the route spatial structures, transport mode choice, and time consumed at each visited vertex. Performance is considerably affected by the first two above-mentioned factors compared with the last, and optimization of time allocation can be considered as an additional step. From this perspective, the evolution of route spatial structure and transport mode choice can serve as a global search, whereas that of time allocation can serve as a local search. With different optimization objectives, these global and local searches lead to varied methods. Spatial structure and transport mode choice are discrete decision variables, so for their evolution, we combine a high learning intensity with individual optimum (σ_1), a low learning intensity with global optimum (σ_2), and a low-frequency DEA. As time allocation is a continuous decision variable, we combine a low σ_1, a high σ_2, and high-frequency DEA for its evolution. The procedure involved in hybrid evolution is shown in Fig. 5.

This procedure emphasizes which search type to adopt. In MOPs, the approach performance is considerably affected by the diversity of solutions in ***POS*** (δ), of which high diversity allows for wider search space for the next iteration. Therefore, the type of search is determined based on the diversity of solutions in ***POS***. If the δ exceeds threshold ξ, then a significantly diverse ***POS***, and even a better one, is available near the solution space (Chen et al., 2015). A local search is more beneficial because a global search may inefficiently seek local solution spaces one after the other (called "jump around"), resulting in poor search performance and convergence. The result likely falls into a local optimum if a significantly diverse ***POS*** is nonexistent ($\delta < \xi$). Here, a global search is more beneficial as "jumping around" local solution spaces increases the possibility of coming across a ***POS*** that is better (Marinakis, Migdalas, & Sifaleras, 2017).

In this step, the δ calculation is clearly one of the most important tasks. The diversity of multi-objective solutions can be measured by variance-based methods or entropy-based methods (Yang et al., 2014). However, these methods cannot evaluate route diversity, which involves discrete and continuous variables. Therefore, the trajectory similarity measuring method proposed by Zheng et al. (2019) is adopted. The method involves earth mover's distance (EMD) and dynamic time warping (DTW), which perform well on in terms of noise resistance and measurement accuracy. The diversity of solutions in ***POS*** can be obtained using Eq. (4.11), where $DisSim\left(PS_i, PS_j\right)$ represents the dissimilarity between solutions PS_i and PS_j (see Zheng et al. (2019)), and P denotes the number of solutions in ***POS***.

$$\delta = \frac{2 \times \sum_{i=1}^{P-1} \sum_{j=i+1}^{P} DisSim\left(PS_i, PS_j\right)}{P \times \left(P-1\right)}, \forall PS_i, PS_j \in \boldsymbol{POS} \quad (4.11)$$

5 Performance evaluation

5.1 Area of the case study

Chengdu, one of the first national historical and cultural cities in China, was selected for the case study. It has a reputation as an established and well-developed urban destination. With its unique, mysterious, and enrichment tourism resources (e.g., natural beauty, historical culture, and gastronomy), Chengdu received over 210 million tourists in 2017, an increase of 10.66% from 2016. Of this number, approximately 130 million tourists took a day tour. Given its many attractions and complex transport system, Chengdu makes itinerary planning extremely challenging. Fig. 6 presents a map of Chengdu City along with the distribution of its 48 chief attractions (represented as black nodes).

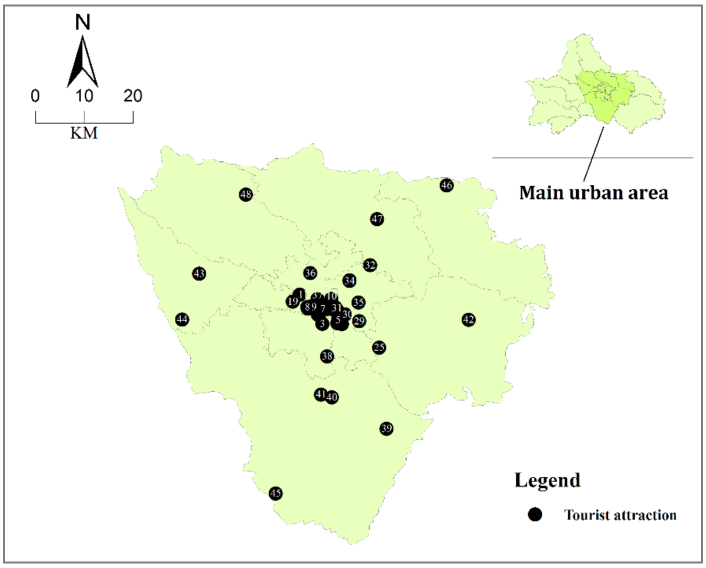

Fig. 6. Chengdu City map

(1) Basic information on the attractions

Among Chengdu's numerous attractions, 48 major attractions were selected for this study based on their popularity and day-tour recommendation ranking in a popular online travel agent (OTA, e.g., Ctrip and Alitrip). Fig. 6 shows the locations of the 48 attractions, and Table 2 (columns 1–4) shows their serial numbers, names, and time windows. At each attraction, the time spent by previous tourists (t_i) profoundly impacts the ***IRS***. Table 2 (column 4) presents data on t_i according to the online reviews shared in the OTA by previous tourists.

Table 2. Basic information on attractions in Chengdu

No.	Name	District	Time window	t_j (min)
a_1	Jinli Street	Wuhou	[00:00–24:00]	1–3 h
a_2	Temple of Marquis Wu	Wuhou	[07:30–21:00]	1–3 h
…..	…..	…..	…..	…..
a_{48}	Three weirs	Pidu	[09:00–21:00]	3–5 h

(2) Travel times between vertices

The main transport modes used by tourists in the main urban area of Chengdu include taxis, the subway, buses, and shared bicycles. Different transport mode choices between attractions result in different travel times. Such travel time is a TDSV, and it depends on the in-between distance and traffic timeslots. For the first quarter of 2019, the Chengdu traffic congestion delay index published by Amap, a popular navigation mobile app similar to Google Map, shows that a workday can be divided into six timeslots, whereas a weekend day has four timeslots. Table 3 lists the detailed timeslots.

Table 3. Chengdu City timeslots

Workday			Weekend		
No.	Timeslot	Traffic congestion delay index	No.	Timeslot	Traffic congestion delay index
TQ_1	[23:00–05:00]	$\lambda \in [0, 1]$	TQ_1	[23:00–08:00]	$\lambda \in [0, 1]$
TQ_2	[05:00–07:30]	$\lambda \in (1, 1.5]$	TQ_2	[08:00–16:00]	$\lambda \in (1, 1.5]$
TQ_3	[07:30–11:00]	$\lambda \in (1.5, 2]$	TQ_3	[16:00–20:00]	$\lambda \in (1.5, 2]$
TQ_4	[11:00–16:00]	$\lambda \in (1, 1.5]$	TQ_4	[20:00–23:00]	$\lambda \in (1, 1.5]$
TQ_5	[16:00–19:00]	$\lambda \in (1.5, 2]$			
TQ_6	[19:00–23:00]	$\lambda \in [0, 1]$			

Determining the distribution functions of travel times between vertices for different transport modes requires considerable data on historical travel times of each transport mode in each timeslot. To this end, data were collected through Amap, which can accurately estimate the travel times for different transport modes in real-time. Specifically, in each timeslot, we input the names of any two vertices in Amap, select one of the traffic modes, and record the corresponding travel time from the Amap outputs. The MATLAB distribution-fitting tool is used for probability density functions. The distribution functions for travel times between vertices are determined for each transport mode in each timeslot. Afterward, the Akaike information criterion (AIC) is utilized to evaluate each distribution's goodness-of-fit and thereby show which is the best. The smaller AIC value, the better the data distribution fit (Xia, Zeephongsekul, & Packer, 2011).

The results are illustrated using the travel time via taxi between Wangjiang Tower Park (a_{23}) and Temple of Marquis Wu (a_2) for TQ_5 ($\tilde{t}_5^1(v_{23}, v_2)$) on a weekday. We collected the taxi time between a_{23} and a_2 in TQ_5 for ten consecutive working days. To improve the efficiency of data collection, we randomly chose five time points in TQ_5 [16:00–19:00] in a day. Thus, fifty historical data of $t_5^1(v_{23}, v_2)$ were collected to fit the probability density functions for $\tilde{t}_5^1(v_{23}, v_2)$. All possible distributions in MATLAB, denoted by corresponding probability density functions, were explored, and the best five are shown in Fig. 7 and Table 4. The best distribution for $\tilde{t}_5(v_{23}, v_2)$ is that of Weibull, which shows the lowest AIC value (Table 4, column 2). Using the same procedure obtained the other five timeslots' best distribution functions. Their probability density functions and corresponding parameters are given in Fig. 8 and Table 5. Similarly, for each timeslot, the probability density functions were determined for travel times between vertices.

Table 4. AIC goodness-of-fit test for each probability density function ($\tilde{t}_5^1(v_{23}, v_2)$)

Distribution	**AIC**	**Number of Parameters**	**Parameters**
Normal	6.577	*2*	(30.94, 6.29)
Nakagami	6.606	*2*	(6.05, 996.26)

Weibull	6.554	2	(33.44, 5.75)
Log-logistic	6.676	2	(3.43, 0.12)
Gamma	6.665	2	(22.27, 1.39)

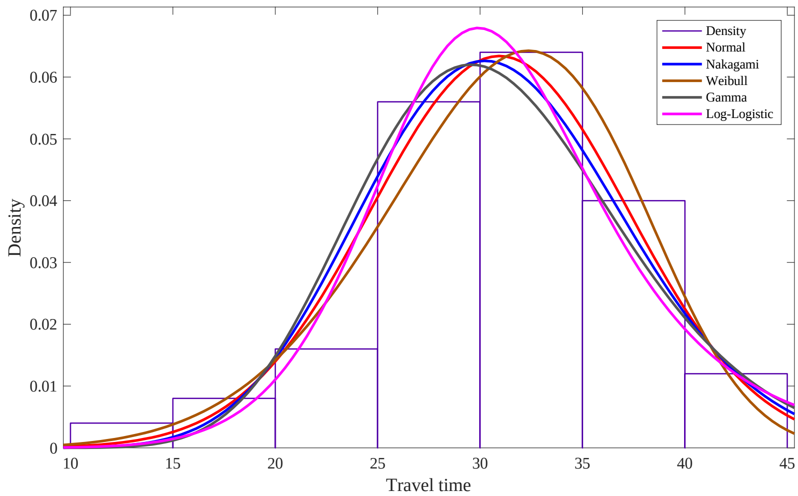

Fig. 7. Probability density functions for $\tilde{t}_5^1(v_{23}, v_2)$

Table 5. Best probability density functions for each timeslot ($\tilde{t}^1(v_{23}, v_2)$)

No.	Timeslot	Best distribution	Parameters
TQ_1	[23:00–05:00]	Gamma	(231.46, 0.07)
TQ_2	[05:00–07:30]	Log-logistic	(3.03, 0.04)
TQ_3	[07:30–11:00]	Gamma	(36.44, 0.87)
TQ_4	[11:00–16:00]	Normal	(20.20, 2.45)
TQ_5	[16:00–19:00]	Weibull	(33.44, 5.75)
TQ_6	[19:00–23:00]	Inverse gaussian	(18.12, 1243.88)

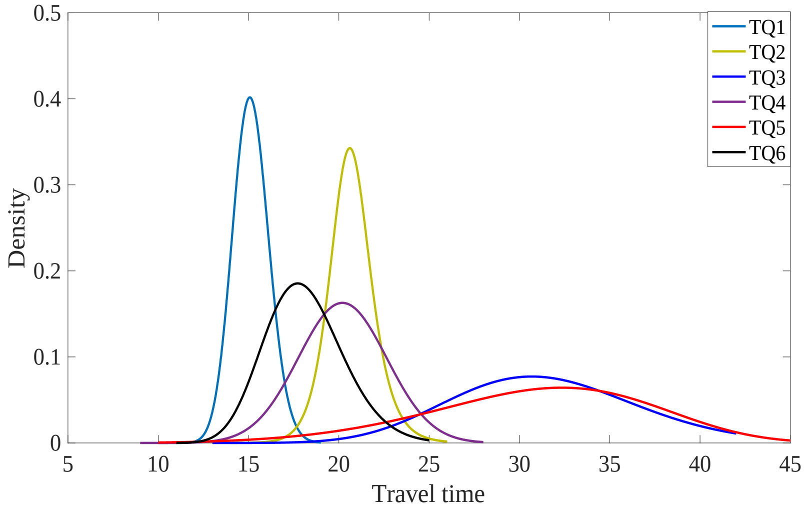

Fig. 8. Probability density functions for $\tilde{t}^1(v_{23}, v_2)$

(3) Basic tourist information

Tourist data were collected at Chengdu Airport (v_{CA}), Chengdu Railway Station (v_{RS}), and Chengdu East Railway Station (v_{ERS}) to retain the sample representativeness. The researchers stood near the exits of the railway stations or the airport and invited the first passenger they came across to participate in the survey. If a passenger refused, the researchers went on to ask the next one until they found a willing participant. The purpose of the passengers' visit to Chengdu was determined through a simple oral interview, and only those passengers who intend to travel within Chengdu were invited to participate in further interviews. Images of the 48 attractions and relevant information were shown to respondents. Subsequently, respondents' starting and ending tour locations and times, "must-visit" and "must-avoid" sites, and preference values for each attraction based on 0 to 1 (1 indicates a high interest for an attraction; 0, no interest in it) were reported. The respondents were likewise asked to rank their attitude toward risk on a scale from 0 to 1 (with 0 indicating complete risk-aversion; 1, high preference for risk). In addition, the respondents also recorded their specific requirements for transport modes: some tourists specified all or a few of the transport modes for their trip, whereas other tourists were flexible with the transport modes. For example, Tourist 15 in Table 6 required using taxis throughout her trip, Tourist 20 preferred to walk from Sichuan University Campus (a_4) to Wangjiang Tower Park (a_{23}) along Funan River, while Tourist 1 was flexible with the transport modes. Of the participants, 21 were male and 29 were female. Collected responses were 23 were at v_{CA}, 12 at v_{RS}, and 15 at v_{ERS}. The aforementioned data gathered from 50 tourists are provided in Table 6.

Table 6. Basic tourist information

Tourist	Gender	Preference Value List	Time Budget	Must-visit Attractions	Attitude toward risk
1	F	[0.94, 0.96, …, 0.18, 0.35]	12 hours	4	0.8
2	M	[0.96, 0.90, …, 0.77, 0.06]	9 hours	None	0.1
…	…	…	…	…	…
50	F	[0.85, 0.72, …, 0.16, 0.75]	8.5 hours	6	0.2

5.2 Algorithm parameters

Optimizing tour routes is considerably influenced by *P*, *G*, learning factors (σ_1 and σ_2), and scale factor (*Fd*). A small *P* increases the possibility of entrapment in the local optimum, but a size too large may result in low computational efficiency. Typically, *G* relies on the convergent situation. A critical parameter that considerably impacts the DEA evolutionary performance is *Fd.* Its best values range from 0.1 to 0.3 (Pal, Saha, & Bandyopadhyay, 2018) to achieve a balance between performance and efficiency. As for PSO learning factors, various MOP studies show that values between 0.5 and 0.9 are the best for σ_1 and σ_2 (Garcia-Gonzalo & Fernández-Martínez, 2012). On the basis of the preceding analysis and real-time scenario in Chengdu, our algorithm parameters are set as follows in Table 7.

Table 7. Algorithm parameters

Parameter	*P*	*G*	*Global search*			*Local search*		
			Improve PSO		*DEA*	*Improve PSO*		*DEA*
			σ_1-*G*	σ_2-*G*	*Fd-G*	σ_1-*G*	σ_2-*G*	*Fd-G*
Value	60	200	0.9	0.5	0.1	0.5	0.9	0.3

5.3 Performance evaluation

Various algorithms commonly used in MOPs serve as baselines for comparison with our approach, such as ant colony optimization (M-ACO), DEA (M-DE), genetic-based algorithm (NSGA-II), particle swarm optimization (M-PSO), and the heuristic approach (NSACDE) proposed by Zheng and Liao (2019). The performance of different methods used in MOPs was evaluated by the inverted generational distance (IGD), which is widely applied (Li & Zhang, 2009) to assess the gap between the true **PF** and the **PF*** obtained by the methods following Eq. (5.1). A smaller IGD value indicates better method performance. A detailed description of IGD is presented by Zheng and Liao (2019). In this evaluation, random errors are reduced by repeating the process 30 times for each tourist and averaging the resultant IGD values. The average IGD values obtained from the six methods are presented in Fig. 9.

$$IGD\left(\boldsymbol{PF^*}, \boldsymbol{PF}_{Ture}\right) = \frac{\sum_{PR \in PF^*} d\left(PR, \boldsymbol{PF}_{Ture}\right)}{\left|\boldsymbol{PF^*}\right|} \tag{5.1}$$

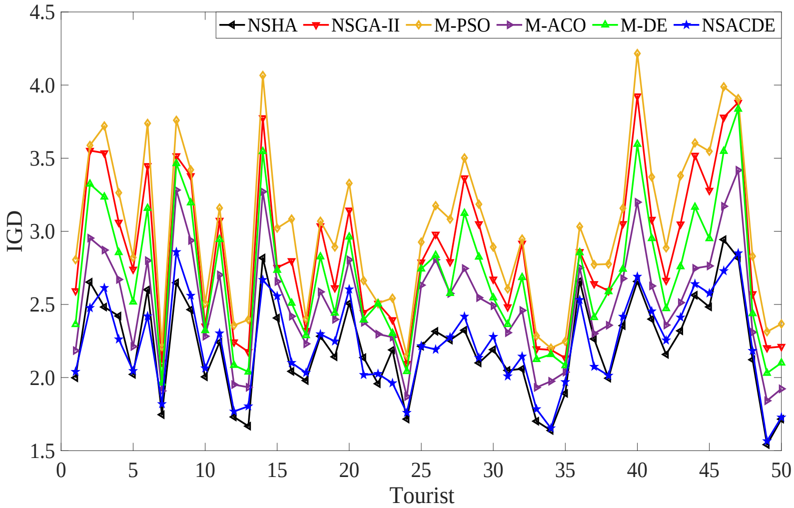

Fig. 9. Average IGD for each tourist (NSHA, NSGA-II, M-PSO, M-ACO, M-DE, and NSACDE)

The performance of the five methods was further analyzed through paired sample *t*-tests to identify which method obtained a smaller IGD. Table 8 presents the mean (*M*) and standard deviations (*SD*) of the IGD obtained using the five algorithms, and Table 9 shows the paired sample *t*-test results. The first pair (NSHA–NSGA-II) shows a gap mean of −0.639, and the IGD obtained using NSHA was significantly smaller (M = 2.212, SD = 0.338) than that obtained using NSGA-II (M = 2.850, SD = 0.515) ($t(50) = -18.181$, $p < 0.05$). Similar results were obtained for the paired sample *t*-test of the second (NSHA–M-PSO), third (NSHA–M-ACO), and fourth (NSHA–M-DE) pairs, indicating that the proposed approach performed significantly better than M-PSO, M-ACO, and M-DE. However, the paired sample *t*-test results for the fifth pair (NSHA–NSACDE) showed no significant difference ($t(50) = -1.235$, $p = 0.223 > 0.05$).

This final result is consistent with the statements in Section 4.3, wherein the comparative analysis between NSACDE and NSHA was conducted. Specifically, NSACDE involves ACO that exposes slow convergence, leading to the algorithm inefficiency in dealing with a TTDP-TMC involving multiple TDSVs (Dorigo & Blum, 2005). Our NSHA combining DEA and an improved PSO is ideally situated for the problem due to its higher search efficiency (Bonyadi & Michalewicz, 2017; Poli, 2008). Therefore, the difference in running time between NSHA and NSACDE is further evaluated. The running time gap mean was −500.48, and the test results revealed that the running time of NSHA was considerably smaller ($M = 608.00$, $SD = 3.88$) than that of NSACDE ($M = 1108.49$, $SD = 5.97$) ($t(50) = -441.68$, $p < 0.05$). From this perspective, although NSHA and NSACDE achieved similar IGD, our NSHA approach was clearly better in terms of computational efficiency.

Table 8. Paired sample statistics

		Mean	N	Std. Deviation	Std. Error Mean
Pair 1	NSHA	2.212	50	0.338	0.048
	NSGA-II	2.850	50	0.515	0.073
Pair 2	NSHA	2.212	50	0.338	0.048
	M-PSO	3.013	50	0.541	0.077
Pair 3	NSHA	2.212	50	0.338	0.048
	M-ACO	2.507	50	0.398	0.056
Pair 4	NSHA	2.212	50	0.338	0.048
	M-DE	2.690	50	0.470	0.066
Pair 5	NSHA	2.212	50	0.338	0.048
	NSACDE	2.230	50	0.323	0.046

Table 9. Paired sample test

	Paired Differences					t	df	Sig. (2-tailed)
	Mean	Std. Deviation	Std. Error Mean	95% Confidence Interval of the Difference				
				Lower	Upper			
Pair 1 NSHA–NSGA-II	-0.639	0.248	0.035	-0.709	-0.568	-18.181	49	0.000***
Pair 2 NSHA–M-PSO	-0.802	0.266	0.038	-0.877	-0.726	-21.302	49	0.000***
Pair 3 NSHA–M-ACO	-0.295	0.128	0.018	-0.331	-0.258	-16.246	49	0.000***
Pair 4 NSHA–M-DE	-0.479	0.202	0.029	-0.536	-0.421	-16.740	49	0.000***
Pair 5 NSHA–NSACDE	-0.018	0.103	0.015	-0.047	0.011	-1.235	49	0.223

*$p < 0.05$; **$p < 0.01$; ***$p < 0.001$.

5.4 Discussion

In Section 5.3, the presented results clearly indicate that our proposed approach realizes the balance between utility and risk better than the current algorithms, and shows excellent performance in computational efficiency. Moreover, with our approach, more multifarious route choices can be designed with the adoption of the Pareto optimality and more sensible and customized routes with the TTDP in a time-dependent stochastic environment that considers spatial-temporal route structure, transport mode choice, and tourist attitude toward risk.

(1) More multifarious route choices

Our approach provides Pareto routes that can meet the diverse preferences of tourists. The first tourist from Table 6 is taken as an example. For this tourist, the allocated time was 12 hours (07:00 to 19:00), and his attitude toward risk is 0.8. A total of 60 routes were designed for this tourist and plotted in Fig. 10 to show the relationship between utility (vertical ordinate) and risk (horizontal ordinate). Measured in probability terms, risk reflects the conservative estimate of completing the trip within the allocated time. A higher risk value indicates a smaller probability of completing the trip within the budget time, and vice versa (Lau et al., 2012). Tourists can then select one of the routes based on the above information. For example, if our tourist focuses on utility, then he will likely choose the first route that has a high utility of 88.41 and a risk value of 0.94. For the tourist to avoid risk as much as possible may therefore prefer the last route, which has a low utility of 64.17 and risk value of 0.45. Apart from these two extremes, 58 other routes were provided to achieve a trade-off between utility and risk.

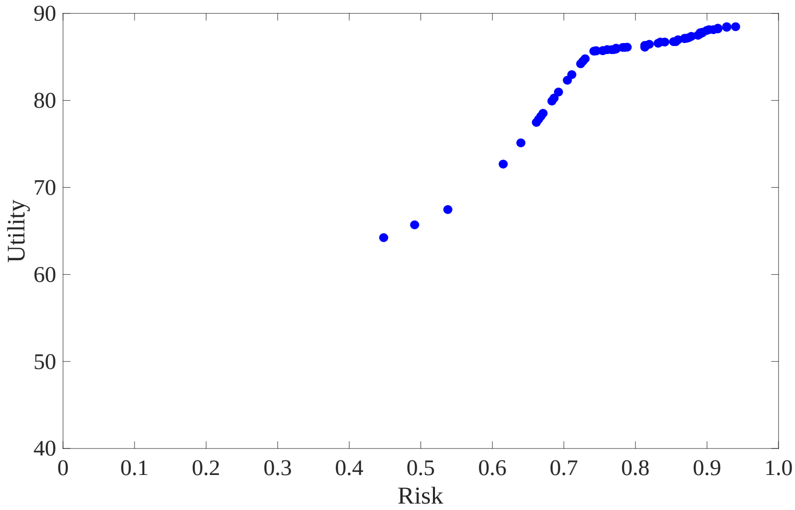

Fig. 10. Routes with relationships between utility and risk (Tourist 1)

(2) More personalized tour routes

A set of routes that can meet diverse choices of tourists can be provided using our approach. In addition, a more personalized set of routes can be generated according to the tourists' risk attitude. A risk-seeking tourist may select a route with greater utility but a higher probability of failure to complete a trip within the allocated time, compared with a risk-averse tourist who may opt for a leisurely pace with lower utility (Lau et al., 2012). Our approach thus involves tourists' attitudes toward risk on top of the personal preferences explored in other studies.

The capability of offering more tailored tour routes can be validated again by selecting Tourist 1 from Table 6 as an example. His actual attitude toward risk is 0.8 (risk-seeking), but was adjusted to 0.2 (risk-averse) and 0.5 (risk-moderate) for comparison. In Fig. 11, the routes shown are designed for the tourist as risk-seeking (blue scatter dots), risk-moderate (green scatter dots), and risk-averse (red scatter dots). The Pareto routes are concentrated as follows for risk-seeking tourists in high-risk and high-utility regions ($\bar{U}$ = 84.15, $\bar{R}$ = 0.79); for risk-averse tourists in low-risk and low-utility regions ($\bar{U}$ = 53.30, $\bar{R}$ = 0.22); and for risk-moderate tourists in a compromise between the two extremes ($\bar{U}$ = 64.45, $\bar{R}$ = 0.47).

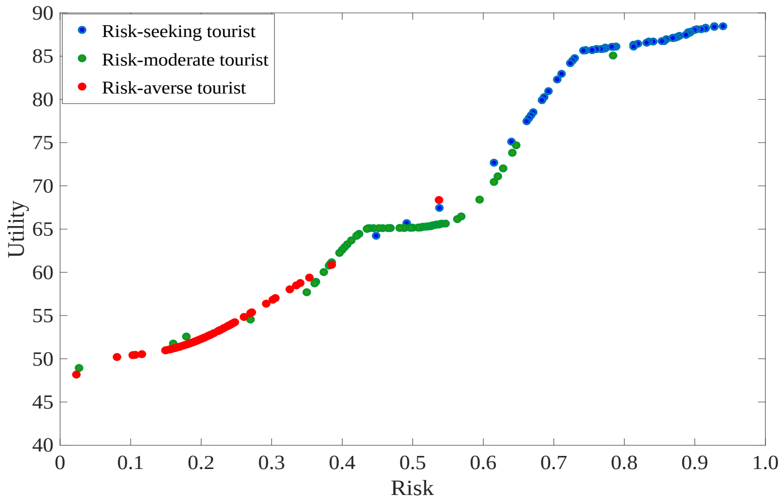

Fig. 11. Routes for tourists with different attitudes toward risk

(3) More sensible tour routes

The multimodal nature of transport systems is rarely considered in designing routes customized for city tourists. Personalized city day tour routes without such considerations are infeasible or suboptimal. A comparative analysis was conducted to explore this issue. Three contrast scenarios were set up for an entire trip: (1) only the taxi is chosen (denoted as "Taxi only"); (2) only the subway is chosen (denoted as "Subway only"); and (3) only the bus is chosen (denoted as "Bus only"). Information from Tourist 1 in Table 6 is taken as an example.

The routes designed for Tourist 1 using our approach are shown in Fig. 12, which considers multimodal transportation transfer (blue scatter dots). The red, yellow, and brown scatter dots denote routes for the first scenario (Taxi only), second scenario (Subway only), and last scenario (Bus only), respectively. Table 10 lists the results of the comparative analysis of the four scenarios, including the maximum (minimum, average) utility and maximum (minimum, average) risk values of the Pareto solutions. As shown in Fig. 12 and Table 10, our method can achieve higher utilities than other scenarios with the same risk, and our approach is less risky than other scenarios with the same utilities.

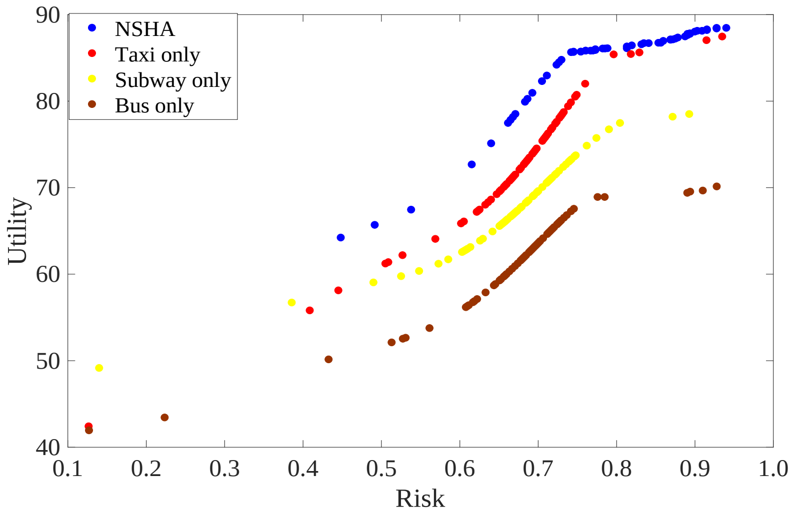

Fig. 12. Routes for tourists with different transportation modes

Table 10. Comparative analysis of the four scenarios

	Mean-Utility	Max-Utility	Min-Utility	Mean-Risk	Max-Risk	Min-Risk
NSHA	84.15	88.41	64.17	0.79	0.94	0.45
Taxi	72.62	87.40	42.35	0.67	0.94	0.13
Subway	68.34	77.07	48.88	0.67	0.93	0.13
Bus	60.80	71.45	42.09	0.67	0.89	0.14

6 Conclusions and future research

The transport system in an urban destination is complex, navigating through it is a big challenge for a tourist, and designing sensible and personalized route recommendations is thus critical for enhancing tourist experience and satisfaction. This study considers transport mode choices and spatial-temporal structures in designing personalized tours. Compared with the general TTDP, our proposed TTDP-TMC is much more advanced due to its optimization of spatial-temporal routes and transport mode choice, and the aim is to gain an advantageous trade-off between utility and risk in a time-dependent stochastic environment. Moreover, our model overcomes the problem of multiple conflicting objectives by adopting the Pareto optimality definition and designing a NSHA with improved PSO and DEA. The illustration case study confirms the superiority of our proposed approach over existing algorithms. Compared with the baseline methods, our model provides more sensible, multifarious, and customized routes for city tourists. Our NSHA could draw considerable interest from the tourism sector practitioners, because of the growing demand for customized experiences in today's tourism market.

This study contributes to tourism research in both methodological and practical fronts. Methodologically, we proposed an effective approach to personalize routes for city tourists. This approach takes into account multiple objectives based on Pareto optimality. Solutions are coded using a triple-layer, variable-length asymmetric chromosome, and they are optimized with discrete and continuous variables combining improved PSO and DEA. Finally, a random simulation-based method is proposed to deal with TDSVs, and a hybrid evolution structure is designed to improve evolutionary efficiency.

Practically, utilizing the latest machine learning and artificial intelligence technologies to provide tourists with personalized tour recommendations will greatly enhance their tourism experience, satisfaction and loyalty, which consequently lead to better business performance for the tourism organization (Piccoli, Lui, & Grün, 2017). The approach proposed in this study further improves the trip design function for the smart tourism recommendation systems, which aims to help tourists to navigate the transport system efficiently. City destination marketing and management organizations could integrate the methodologies and algorithms proposed in this study to upgrade their tour recommendation systems as part of their e-business or digital transformation strategy to enhance the destinations' services, thereby helping them gain a competitive edge in the market (Edwards, Griffin, & Hayllar, 2008). Independent tourists can utilize the recommendation system designed using our approach when planning their tour routes in the urban context. This ideal scenario promises enhanced travel experiences.

Further research could tackle the problem of designing personalized itineraries in a multi-day tour context with consideration of both hotel selection and transport mode choice. Many city tourism attractions can be abstracted as vertices or arcs (e.g., coastline, greenway, river, and street). As the tourists' utility is associated both arcs and vertices, future researchers could combine OP and arc routing problems with profits to come up with tour itineraries for urban tourists. Finally, it would be valuable and promising to design a highly robust travel route recommendation system that can adapt to the dynamic adjustment of the tourists who may want change routes away from the recommended options during their trips.

References

Abbaspour, R. A., & Samadzadegan, F. (2011). Time-dependent personal tour planning and scheduling in metropolises. *Expert Systems with Applications, 38*(10), 12439-12452.

Albalate, D., & Bel, G. (2010). Tourism and urban public transport: Holding demand pressure under supply constraints. *Tourism Management, 31*(3), 425-433.

Ashworth, G., & Page, S. J. (2011). Urban tourism research: Recent progress and current paradoxes. *Tourism Management, 32*(1), 1-15.

Bonyadi, M. R., & Michalewicz, Z. (2017). Particle swarm optimization for single objective continuous space problems: A review. *Evolutionary Computation, 25*(1), 1-54.

Chen, B., Lin, Y., Zeng, W., Zhang, D., & Si, Y.-W. (2015). Modified differential evolution algorithm using a new diversity maintenance strategy for multi-objective optimization problems. *Applied Intelligence, 43*(1), 49-73.

Chen, Z., Zhou, Y., & Xiang, Y. (2017). A many-objective evolutionary algorithm based on a projection-assisted intra-family election. *Applied Soft Computing, 61*, 394-411.

Chi, C. G.-Q., & Qu, H. (2008). Examining the structural relationships of destination image, tourist satisfaction and destination loyalty: An integrated approach. *Tourism Management, 29*(4), 624-636.

Debbage, K. G. (1991). Spatial behavior in a bahamian resort. *Annals of Tourism Research, 18*(2), 251-268.

Dejbakhsh, S., Arrowsmith, C., & Jackson, M. (2011). Cultural influence on spatial behaviour. *Tourism Geographies, 13*(1), 91-111.

Dorigo, M., & Blum, C. (2005). Ant colony optimization theory: A survey. *Theoretical Computer Science, 344*(2), 243-278.

Edwards, D., Griffin, T., & Hayllar, B. (2008). Urban tourism research: Developing an agenda. *Annals of Tourism Research, 35*(4), 1032-1052.

Fennell, D. A. (1996). A tourist space-time budget in the shetland islands. *Annals of Tourism Research, 23*(4), 811-829.

Forgas-Coll, S., Palau-Saumell, R., Sánchez-García, J., & Callarisa-Fiol, L. J. (2012). Urban destination loyalty drivers and cross-national moderator effects: The case of barcelona. *Tourism Management, 33*(6), 1309-1320.

Garcia-Gonzalo, E., & Fernández-Martínez, J. L. (2012). A brief historical review of particle swarm optimization (pso). *Journal of Bioinformatics and Intelligent Control, 1*(1), 3-16.

Garcia, A., Vansteenwegen, P., Arbelaitz, O., Souffriau, W., & Linaza, M. T. (2013). Integrating public transportation in personalised electronic tourist guides. *Computers & Operations Research, 40*(3), 758-774.

Gavalas, D., Kasapakis, V., Konstantopoulos, C., Pantziou, G., Vathis, N., & Zaroliagis, C. (2015). The ecompass multimodal tourist tour planner. *Expert Systems with Applications, 42*(21), 7303-7316.

Gavalas, D., Konstantopoulos, C., Mastakas, K., Pantziou, G., & Vathis, N. (2015). Heuristics for the time dependent team orienteering problem: Application to tourist route planning. *Computers & Operations Research, 62*(10), 36-50.

Gretzel, U. (2011). Intelligent systems in tourism: A social science perspective. *Annals of Tourism Research, 38*(3), 757-779.

Gretzel, U., Sigala, M., Xiang, Z., & Koo, C. (2015). Smart tourism: Foundations and developments. *Electronic Markets*, *25*(3), 179-188.

Gronau, W. (2017). On the move: Emerging fields of transport research in urban tourism. In N. Bellini & C. Pasquinelli (Eds.), *Tourism in the city : Towards an integrative agenda on urban tourism* (pp. 81-91). Cham: Springer International Publishing.

Hyde, K. F., & Laesser, C. (2009). A structural theory of the vacation. *Tourism Management, 30*(2), 240-248.

Kaul, R. N. (1985). *Dynamics of tourism: A trilogy. Transportation and marketing*: Sterling Publishers.

Kennedy, J., & Eberhart, R. (1995). *Particle swarm optimization.* Paper presented at the Proceedings of the IEEE International Conference on Neural Networks.

Kotiloglu, S., Lappas, T., Pelechrinis, K., & Repoussis, P. P. (2017). Personalized multi-period tour recommendations. *Tourism Management*, *62*(5), 76-88.

Lau, H. C., Yeoh, W., Varakantham, P., Nguyen, D. T., & Chen, H. (2012). *Dynamic stochastic orienteering problems for risk-aware applications*. Paper presented at the Proceedings of the Twenty-Eighth Conference on Uncertainty in Artificial Intelligence.

Le-Klähn, D.-T., Roosen, J., Gerike, R., & Hall, C. M. (2015). Factors affecting tourists' public transport use and areas visited at destinations. *Tourism Geographies*, *17*(5), 738-757.

Lee, D., & Hosanagar, K. (2019). How do recommender systems affect sales diversity? A cross-category investigation via randomized field experiment. *Information Systems Research*, *30*(1), 239-259.

Lew, A., & McKercher, B. (2006). Modeling tourist movements: A local destination analysis. *Annals of Tourism Research, 33*(2), 403-423.

Li, H., & Zhang, Q. (2009). Multiobjective optimization problems with complicated pareto sets, moea/d and nsga-ii. *IEEE Transactions on Evolutionary Computation, 13*(2), 284-302.

Li, Y., Hu, C., Huang, C., & Duan, L. (2017). The concept of smart tourism in the context of tourism information services. *Tourism Management*, *58*, 293-300.

Liao, Z., & Zheng, W. (2018). Using a heuristic algorithm to design a personalized day tour route in a time-dependent stochastic environment. *Tourism Management, 68*(5), 284-300.

Lim, K. H., Chan, J., Karunasekera, S., & Leckie, C. (2019). Tour recommendation and trip planning using location-based social media: A survey. *Knowledge and Information Systems, 60*(3), 1247-1275.

Lin, Z., He, G., & Vlachos Ilias, P. (2015). Britain in bloom? A study into chinese tourists' experience. *EuroMed Journal of Business, 10*(3), 297-310.

Lin, Z., Vlachos, I., & Ollier, J. (2018). Prioritizing destination attributes for optimal resource allocation: A study of chinese tourists visiting britain. *Journal of Travel*

& Tourism Marketing, 35(8), 1013-1026.

Marinakis, Y., Migdalas, A., & Sifaleras, A. (2017). A hybrid particle swarm optimization–variable neighborhood search algorithm for constrained shortest path problems. *European Journal of Operational Research, 261*(3), 819-834.

Masiero, L., & Zoltan, J. (2013). Tourists intra-destination visits and transport mode: A bivariate probit model. *Annals of Tourism Research, 43*, 529-546.

McKercher, B., Shoval, N., Ng, E., & Birenboim, A. (2012). First and repeat visitor behaviour: Gps tracking and gis analysis in hong kong. *Tourism Geographies, 14*(1), 147-161.

Osman, M. S., Abo-Sinna, M. A., & Mousa, A. A. (2005). An effective genetic algorithm approach to multiobjective resource allocation problems (moraps). *Applied Mathematics & Computation, 163*(2), 769-781.

Pal, M., Saha, S., & Bandyopadhyay, S. (2018). Decor: Differential evolution using clustering based objective reduction for many-objective optimization. *Information Sciences, 423*, 200-218.

Parouha, R. P., & Das, K. N. (2016). A robust memory based hybrid differential evolution for continuous optimization problem. *Knowledge-Based Systems, 103*(7), 118-131.

Pellegrini, A., & Scagnolari, S. (2019). The relationship between length of stay and land transportation mode in the tourism sector: A discrete–continuous framework applied to swiss data. *Tourism Economics*, 1354816619891320.

Piccoli, G., Lui, T.-W., & Grün, B. (2017). The impact of it-enabled customer service systems on service personalization, customer service perceptions, and hotel performance. *Tourism Management, 59*(2), 349-362.

Plog, S. C. (2002). The power of psychographics and the concept of venturesomeness. *Journal of Travel Research, 40*(3), 244-251.

Poli, R. (2008). Analysis of the publications on the applications of particle swarm optimisation. *Journal of Artificial Evolution Applications, 2008*(1), 1-10.

Prideaux, B. (2000). The role of the transport system in destination development. *Tourism Management, 21*(1), 53-63.

Rodríguez, B., Molina, J., Pérez, F., & Caballero, R. (2012). Interactive design of personalised tourism routes. *Tourism Management, 33*(4), 926-940.

Tsai, C.-Y., & Chung, S.-H. (2012). A personalized route recommendation service for theme parks using rfid information and tourist behavior. *Decision Support Systems, 52*(2), 514-527.

Tussyadiah, I. (2020). A review of research into automation in tourism: Launching the annals of tourism research curated collection on artificial intelligence and robotics in tourism. *Annals of Tourism Research, 81*, 102883.

Vansteenwegen, P., & Van Oudheusden, D. (2007). The mobile tourist guide: An or opportunity. *OR Insight*, *20*(3), 21-27.

Verbeeck, C., Vansteenwegen, P., & Aghezzaf, E. H. (2016). Solving the stochastic time-dependent orienteering problem with time windows. *European Journal of Operational Research*, *255*(3), 699-718.

Wang, X., Li, X., Zhen, F., & Zhang, J. (2016). How smart is your tourist attraction?: Measuring tourist preferences of smart tourism attractions via a fcem-ahp and ipa approach. *Tourism Management, 54*(3), 309-320.

Wong, C. U. I., & McKercher, B. (2012). Day tour itineraries: Searching for the balance between commercial needs and experiential desires. *Tourism Management, 33*(6), 1360-1372.

Xia, J. C., Evans, F. H., Spilsbury, K., Ciesielski, V., Arrowsmith, C., & Wright, G. (2010). Market segments based on the dominant movement patterns of tourists. *Tourism Management, 31*(4), 464-469.

Xia, J. C., Zeephongsekul, P., & Packer, D. (2011). Spatial and temporal modelling of tourist movements using semi-markov processes. *Tourism Management, 32*(4), 844-851.

Yang, M., Li, C., Cai, Z., & Guan, J. (2014). Differential evolution with auto-enhanced population diversity. *IEEE Transactions on Cybernetics, 45*(2), 302-315.

Yin, P., Lin, Z., & Prideaux, B. (2019). The impact of high-speed railway on tourism spatial structures between two adjoining metropolitan cities in china: Beijing and tianjin. *Journal of Transport Geography, 80*, 102495.

Zheng, W., Ji, H., Lin, C., Wang, W., & Yu, B. (2020). Using a heuristic approach to design personalized urban tourism itineraries with hotel selection. *Tourism Management, 76*(1), 1-14.

Zheng, W., & Liao, Z. (2019). Using a heuristic approach to design personalized tour routes for heterogeneous tourist groups. *Tourism Management, 72*(3), 313-325.

Zheng, W., Liao, Z., & Qin, J. (2017). Using a four-step heuristic algorithm to design personalized day tour route within a tourist attraction. *Tourism Management, 62*(5), 335-349.

Zheng, W., Zhou, R., Zhang, Z., Zhong, Y., Wang, S., Wei, Z., & Ji, H. (2019). Understanding the tourist mobility using GPS: How similar are the tourists? *Tourism Management, 71*(2), 54-66.